Stability of nonlinear waves: pointwise estimates

Margaret Beck

July 24, 2015

Abstract

This is an expository article containing a brief overview of key issues related to the stability of nonlinear waves, an introduction to a particular technique in stability analysis known as pointwise estimates, and two applications of this technique: time-periodic shocks in viscous conservation laws [BSZ10] and source defects in reaction diffusion equations [BNSZ12, BNSZ14].

1 Introduction to stability analysis for nonlinear waves

We begin with a brief overview of key issues related to the stability of nonlinear waves. A nonlinear wave is any type of wave, pattern, or other permanent structure that exists as a solution of a mathematical model of a physical system. Ideally, analysis of such a model would help one understand and predict the evolution of the real physical system. One important aspect of this is stability. Roughly speaking, a solution is stable if any other solutions that start near it stay near it for all time, and maybe even converge to it as time tends to infinity. Stable solutions are important because typically it is only stable solutions that are observable in the real world. If the system state is near an unstable solution, than any natural fluctuations in the system lead to evolution away from the unstable solution, towards a stable one.

The basic setup is to begin with a nonlinear partial differential equation (PDE) of the form

$$u_t = \mathcal{F}(u), \tag{1.1}$$

where $u = u(x,t)$ for $x \in \Omega \subseteq \mathbb{R}^d$ and Ω is some specified spatial domain. Typically we will take $\Omega = \mathbb{R}$. The function $\mathcal{F}$ denotes all terms – linear, nonlinear, differential, etc - in the equation other than the time-derivative term u_t. Note this does not require that the PDE be first order in time. For example, the wave equation $v_{tt} = v_{xx}$ can be cast in the above form via

$$\frac{\partial}{\partial t}\begin{pmatrix} v \\ w \end{pmatrix} = \begin{pmatrix} 0 & 1 \\ \partial_x^2 & 0 \end{pmatrix}\begin{pmatrix} v \\ w \end{pmatrix},$$

where we then take $u = (v, w)$ and the right hand side of the above equation to be $\mathcal{F}(u)$. Typical examples of such PDEs that appear in the nonlinear waves literature are

$$u_t = u_{xx} + f(u), \qquad u_t = -u_{xxx} - u^p u_x, \qquad u_t = \mathrm{i}(u_{xx} - \omega u + u|u|^2),$$

which are a reaction-diffusion equation, the Korteweg-deVries (KdV) equation, and the Schrödinger equation, respectively.

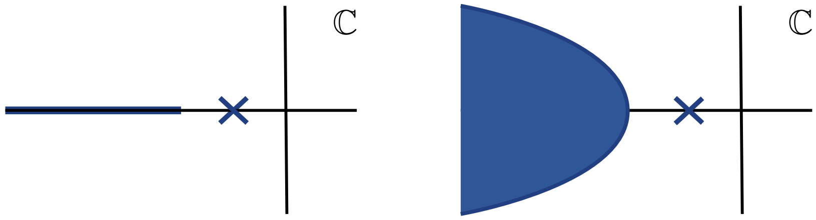

Figure 1: Typical spectra of linear operators that are spectrally stable in a strong sense: $\sup \mathrm{Re}\sigma(\mathcal{L}) < 0$. On the left we see a half line of essential spectrum and an isolated eigenvalue (the cross), and on the right we see a parabolic region of essential spectrum and an isolated eigenvalue.

Suppose $u^*(x)$ is the nonlinear wave whose stability we wish to study. We assume for simplicity that it is stationary solution, meaning that it is independent of time and $0 = u^*_t = \mathcal{F}(u^*)$. (This stationarity condition will be relaxed below to allow for traveling and time-periodic waves.) One then makes the following Ansatz. Assume the solution to (1.1) has the form

$$u(x,t) = u^*(x) + p(x,t), \tag{1.2}$$

where $p(x,t)$ is thought of as the perturbation of the wave u^*. We also assume that $p(x,0)$ is small in some appropriate norm, so that the solution u starts near the wave u^*. Inserting (1.2) into (1.1), we find

$$p_t = u_t = \mathcal{F}(u) = \mathcal{F}(u^* + p) = \mathcal{F}(u^*) + D\mathcal{F}(u^*)p + [\mathcal{F}(u^* + p) - \mathcal{F}(u^*) - D\mathcal{F}(u^*)p] = D\mathcal{F}(u^*)p + \mathcal{N}(p)$$

where the nonlinear term satisfies $\mathcal{N}(p) = \mathcal{F}(u^* + p) - D\mathcal{F}(u^*)p = \mathcal{O}(p^2)$, assuming that F is smooth in some appropriate sense, and we have used the fact that $0 = \mathcal{F}(u^*)$. Thus, the evolution of the perturbation is governed by

$$p_t = \mathcal{L}p + \mathcal{N}(p), \qquad \mathcal{L} = D\mathcal{F}(u^*) \tag{1.3}$$

where the linear operator $\mathcal{L}$ is the linearization of the original PDE about the solution of interest.

The reason for separating (1.3) into its linear and nonlinear parts is that, when p is small, which we expect to be true at least for small times since $p(x,0)$ is small, the nonlinear terms will be much smaller than the linear terms, because $p^2 \ll |p|$ for $|p| \ll 1$. Thus, we expect the linear equation $p_t = \mathcal{L}p$, and in particular the spectrum of the operator $\mathcal{L}$, to provide key insights into whether the perturbation will grow or decay. This is analogous with the way one studies the stability of a fixed point of an ordinary differential equation (ODE): one linearizes the ODE at the fixed point to determine a matrix, or linear operator, known as the Jacobian, and then the eigenvalues of that matrix are used to determine the stability of the fixed point. The same general strategy will be applied here as in the ODE case, but there are several complications that arise due to the fact that (1.3) typically has an infinite-dimensional phase space, rather than the finite-dimensional one that an ODE has. As a result, this type of PDE analysis is sometimes characterized as the study of infinite-dimensional dynamical systems.

We now outline three key steps in analyzing the stability of u^* via the equation (1.3): determining spectral stability, linear stability, and nonlinear stability. The wave u^* is said to be spectrally stability if $\mathcal{L}$ has no spectrum, which we denote by $\sigma(\mathcal{L})$, with positive real part. Figure 1 shows typical spectra of linear operators with $\sup \mathrm{Re}\sigma(\mathcal{L}) < 0$. This type of spectral picture suggests a strong type of stability, known as asymptotic stability, in which the perturbation decays to zero as time goes to infinity. Continuing the

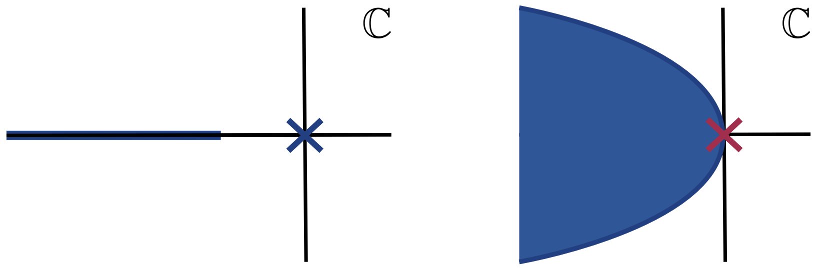

Figure 2: Typical spectra of linear operators that are spectrally stable in a weaker sense: $\sup \mathrm{Re}\sigma(\mathcal{L}) = 0$. On the left we see a half line of essential spectrum and an isolated eigenvalue (the cross) on the imaginary axis, and on the right we see a parabolic region of essential spectrum touching the imaginary axis and an embedded eigenvalue (denoted now in red for visual clarity) at the origin.

analogy withe ODEs, this would correspond to a fixed point whose Jacobian has only eigenvalues with negative real part. One key difference between linear operators in infinite dimensions and those in finite dimensions is that, in the latter case, the spectrum just consists of eigenvalues, whereas in the former case, there can be both eigenvalues (also referred to as point spectrum) and also essential spectrum. The essential spectrum will not be discussed in detail here, but it can be thought of loosely as the part of the spectrum that does not just consist of isolated points. (This is also sometimes referred to as continuous spectrum, but that is typically a less precise term.) See [KP13] for more details.

On the other hand, Figure 2 shows typical spectra of linear operators with $\sup \mathrm{Re}\sigma(\mathcal{L}) = 0$. This is a slightly weaker type of spectral stability that is consistent with the perturbation remaining small for all time. The analogy from ODEs would be a fixed point whose Jacobian has an eigenvalue with zero real part. In this case, in order to prevent algebraic growth of perturbations, one would need the geometric and algebraic multiplicities of this eigenvalue to be equal. The right panel of Figure 2 shows a situation that does not occur for ODEs, because a matrix does not have essential spectrum. In this example, the operator is said to lack a spectral gap, because there is no gap between the continuous spectrum and the eigenvalue at zero; the eigenvalue is embedded in the continuous spectrum. We will return to this issue below.

Of course one could also have a spectrum that extends into the open right half plane. This would suggest that there would be perturbations that would grow exponentially fast, and thus the underlying wave would be unstable. For more information about the spectral stability of operators that result from linearization about a nonlinear wave, see [KP13].

Consider now linear stability. This refers to the behavior of solutions of the linear equation

$$p_t = \mathcal{L}p.$$

If this were an ODE, and $\mathcal{L}$ were a matrix, then the behavior of solutions would be completely determined by the eigenvalues (and eigenvectors) of $\mathcal{L}$. Thus, in finite dimensions, spectral and linear stability are equivalent. In other words, if all eigenvalues have negative real part, then solutions to the linear equation will decay exponentially fast, and so, at the linear level, the underlying wave is asymptotically stable. In addition, if all eigenvalues have nonpositive real part, and the algebraic and geometric multiplicities of any eigenvalues with zero real part are equal, then solutions to the linear equation will remain bounded for all time. Hence, at the linear level the underlying wave would be what's referred to as Lyapunov stable. To prove this, one could use the fact that solutions to the linear equation are given by the matrix exponential: $p(t) = e^{\mathcal{L}t}p(0)$. In finite dimensions, this exponential operator, known as a semigroup, satisfies a so-called spectral mapping theorem: $\sigma(e^{\mathcal{L}}) \setminus \{0\} = e^{\sigma(\mathcal{L})}$.

In infinite-dimensions the situation is more subtle. One issue is that the semigroup $e^{\mathcal{L}t}$ is not well defined for arbitrary operators $\mathcal{L}$. (Although this will not really be an issue for the operators considered below.) Moreover, is possible for $\sup \mathrm{Re}\sigma(\mathcal{L}) < 0$, but for $p_t = \mathcal{L}p$ to have solutions that grow exponentially fast as t increases. In other words, $e^{\mathcal{L}}$ fails to satisfy the spectral mapping theorem described above. Associated to any semigroup are the spectral and growth bounds, defined respectively as

$$\delta = \sup \mathrm{Re}\sigma(\mathcal{L}), \qquad \omega_0 = \inf\{\omega : \exists C(\omega) \text{ such that } \|e^{\mathcal{L}t}\| \le Ce^{\omega t}\}.$$

One can prove that $\delta \le \omega$, but it is possible for $\delta < \omega$. An example of such an operator is given by $\mathcal{L} = x\partial_x$ on the space $H^1(1,\infty)$. One can show explicitly that $\sup \mathrm{Re}\sigma(\mathcal{L}) = -1/2$, but there exist solutions such that $\|p(t)\|_{H^1(1,\infty)} \ge Ce^{t/2}$. Note that the fact that $\delta < \omega$ implies that, if there is spectrum with positive real part, then there exist solutions to the linear equation that grow exponentially fast, and hence the underlying wave in linearly unstable. For more information on semigroups and spectral mapping theorems, see [EN00, Paz83].

Another difference between linear stability in finite and infinite dimensions is due to the continuous spectrum and possible lack of a spectral gap. In an example such as the right panel of Figure 2, even if it is known that the geometric and algebraic multiplicities of the eigenvalue at zero are equal, it's not clear that there cannot be some interaction between this eigenvalue and the continuous spectrum that would lead to the growth of solutions to the linear equation. Thus, in a situation where the continuous spectrum touches the imaginary axis, one needs more information in order to determine linear stability. We also note that, if there is spectrum touching the imaginary axis (and there are no eigenvalues on the imaginary axis), one can still have decay of perturbations to zero as $t \to \infty$. In this case, however, one typically expects the perturbations to decay only algebraically, rather than exponentially.

Finally, we turn to nonlinear stability. This is the most relevant for applications, as it takes all terms of equation (1.3) into account. Often one can use Duhamel's formula, also known as variation of parameters,

$$p(t) = e^{\mathcal{L}t}p(0) + \int_0^t e^{\mathcal{L}(t-s)}\mathcal{N}(p(s))\mathrm{d}s, \tag{1.4}$$

which gives an implicit representation of solutions to (1.3). If $\|e^{\mathcal{L}t}\| \le Ce^{\omega t}$ for some $\omega < 0$ and the nonlinearity is well-behaved, then (1.4) and an estimate like Gronwall's inequality can be used to prove that $\|p(t)\| \le Ce^{\omega t}$, as well. If there are eigenvalues on the imaginary axis and a spectral gap, such as the left panel of Figure 2, then one can, for example, use spectral projections and center manifold theory to determine nonlinear stability, just as one would do in finite dimensions. See [Hen81] for more details. If there is no spectral gap, as in the right panel of Figure 2, then there are no general methods for determining nonlinear stability. This is arguably the most challenging and the most interesting situation from a mathematical perspective.

Remark 1.1. *Although the above framework is useful for studying the evolution of a wide variety of physical models, there are certainly many PDEs for which completely different techniques are required. There are*

PDEs for example that are highly nonlinear and such that ignoring any nonlinear terms does not give a good first approximation of the expected behavior. Moreover, the above framework requires that the linear operator $\mathcal{L}$ be nice enough so that the semigroup $e^{\mathcal{L}t}$ is well defined. If this fails, other methods will likely be more useful.

2 Introduction to pointwise estimates

2.1 Main idea at the linear level

Pointwise estimates are one method that can be useful for stability analysis in the case where there does not exist a spectral gap. This method was initially developed in [ZH98] and further refined in a variety of papers by Zumbrun and various coauthors. See [Zum11] for a relatively basic treatment of the general method.

To illustrate the basic idea involved, consider the following spectral problem. Fix a linear operator $\mathcal{L}$ and a complex number λ. Given any function f (in some appropriate function space), can we solve

$$(\lambda - \mathcal{L})p = f$$

for the unknown function p (also in an appropriate function space)? If so we say that λ is in the resolvent set of $\mathcal{L}$: $\lambda \in \rho(\mathcal{L})$. If not, we say that λ is in the spectrum of $\mathcal{L}$: $\lambda \in \sigma(\mathcal{L})$. Note that we need to be able to solve the above equation for all f in order for $\lambda \in \rho(\mathcal{L})$. Suppose $G(x, y, \lambda)$ is a function that satisfies

$$(\lambda - \mathcal{L})G = \delta(x - y),$$

where δ is the Dirac delta function centered at $x = y$. One can then check that $p(x, \lambda) = \int G(x, y, \lambda)f(y)\mathrm{d}y$ is the desired solution. The function G is called the resolvent kernel. It is an integral kernel that describes the action of the resolvent operator $(\lambda - \mathcal{L})^{-1}$. Note that G is defined pointwise in (x, y, λ).

Consider now the linear equation $p_t = \mathcal{L}p$ and recall that the Laplace transform is defined via

$$\tilde{p}(\lambda) = \int_0^\infty e^{-\lambda t}p(t)\mathrm{d}t.$$

If we take the Laplace transform of $p_t = \mathcal{L}p$, we find $(\lambda - \mathcal{L})\tilde{p} = p(0)$. Solving for $\tilde{p}$ and inverting the Laplace transform, we find

$$p(t) = \frac{1}{2\pi\mathrm{i}}\int_\Gamma e^{\lambda t}(\lambda - \mathcal{L})^{-1}p(0)\mathrm{d}\lambda,$$

where Γ is a contour in the complex plane that does not intersect the spectrum of $\mathcal{L}$ (so that $(\lambda - \mathcal{L})^{-1}$ is well-defined on Γ) and extends to infinity in such a way that the above integral is convergent. Note that the above formula is just the usual contour integral representation of the semigroup:

$$p(t) = e^{\mathcal{L}t}p(0), \qquad e^{\mathcal{L}t} = \frac{1}{2\pi\mathrm{i}}\int_\Gamma e^{\lambda t}(\lambda - \mathcal{L})^{-1}\mathrm{d}\lambda.$$

If we now replace the resolvent operator with the resolvent kernel in the above formulas, we obtain a pointwise representation of the linear evolution:

$$p(x, t) = \int_{\mathbb{R}} \mathcal{G}(x, y, t)p(y, 0)\mathrm{d}y, \qquad \mathcal{G}(x, y, t) = \frac{1}{2\pi\mathrm{i}}\int_\Gamma e^{\lambda t}G(x, y, \lambda)\mathrm{d}\lambda. \tag{2.1}$$

The function $\mathcal{G}$ is known as the pointwise Greens function; it is a pointwise representation of the semigroup.

As an example, consider $\mathcal{L} = \partial_x^2$, so our linear equation is just the one-dimensional heat equation on the real line. On the space $L^2(\mathbb{R})$, this operator has spectrum given by $(-\infty, 0]$ (which consists entirely of essential spectrum). The resolvent kernel and Greens function are given by

$$G(x, y, \lambda) = \frac{1}{2\sqrt{\lambda}} e^{-\sqrt{\lambda}|x-y|}, \qquad \mathcal{G}(x, y, t) = \frac{1}{\sqrt{4\pi t}} e^{-\frac{(x-y)^2}{4t}}.$$

Note that one can "see" the spectrum in the resolvent kernel, in that it does not decay at spatial infinity for $\lambda \in (-\infty, 0]$. For such λ, integration against G is not a well-behaved map from $L^2(\mathbb{R})$ to itself. Moreover, the Greens function is just the usual heat kernel. It decays only algebraically in time, which is expected as there is no gap between the essential spectrum and the imaginary axis.

As another example, consider Burgers equation and its viscous shock

$$u_t = u_{xx} - u u_x, \qquad u^*(x) = -\tanh(x/2), \qquad x \in \mathbb{R}.$$

Stability is then determined by

$$p_t = \mathcal{L}p - p p_x, \qquad \mathcal{L}p = p_{xx} + \tanh\left(\frac{x}{2}\right) p_x + \frac{1}{2}\mathrm{sech}^2\left(\frac{x}{2}\right) p. \tag{2.2}$$

One can show that the spectrum of the linear operator is given by the parabolic region $\sigma(\mathcal{L}) = \{\lambda \in \mathbb{C} : \mathrm{Re}(\lambda) \leq -(\mathrm{Im}(\lambda))^2\}$. In addition, there is an embedded eigenvalue at $\lambda = 0$ with eigenfunction $u_x^*(x)$. Thus, qualitatively it looks like the picture in Figure 2 on the right. One can also solve explicitly for the resolvent kernel to find

$$G(x, y, \lambda) = \frac{1}{2\lambda\sqrt{\lambda + \frac{1}{4}}} e^{-\sqrt{\lambda+\frac{1}{4}}|x-y|} \mathrm{sech}\left(\frac{x}{2}\right) \mathrm{sech}\left(\frac{y}{2}\right) g\left(x, y, \sqrt{\lambda + \frac{1}{4}}\right),$$

where

$$\begin{aligned} g\left(x, y, \sqrt{\lambda + \frac{1}{4}}\right) &= \left[\frac{1}{2}\tanh\left(\frac{x}{2}\right) + \sqrt{\lambda + \frac{1}{4}}\right]\left[-\frac{1}{2}\tanh\left(\frac{y}{2}\right) + \sqrt{\lambda + \frac{1}{4}}\right] H(x-y) \\ &\quad + \left[\frac{1}{2}\tanh\left(\frac{y}{2}\right) + \sqrt{\lambda + \frac{1}{4}}\right]\left[\frac{1}{2}\tanh\left(\frac{x}{2}\right) + \sqrt{\lambda + \frac{1}{4}}\right] H(y-x) \end{aligned}$$

and H is the Heaviside function.

The key point is that, although $(\lambda - \mathcal{L})^{-1}$ is not well-defined if $\lambda \in \sigma(\mathcal{L})$, the resolvent kernel G is not too badly behaved if $\lambda \in \sigma(\mathcal{L}) \setminus (-\infty, -1/4]$. This is important because the spectrum implies that the growth bound for the semigroup is no smaller than 0, and so the best bound on the semigroup one can hope for is $\|e^{\mathcal{L}t}\| \leq C$. However, using the pointwise representation (2.1), one could potentially deform the contour Γ into the essential spectrum in some appropriate way and prove that the linear evolution decays algebraically. (There is an issue with the eigenvalue at zero; we will return to this, below.) One can think of this in terms of how one can "see" the spectrum in the resolvent kernel. In this case, the branch cut $(-\infty, -1/4]$ corresponds to something called the absolute spectrum (see [KP13]). The pole at $\lambda = 0$ corresponds to the eigenvalue at zero. Finally the rest of the spectrum corresponds to values of λ for which $|e^{-\sqrt{\lambda+\frac{1}{4}}|z|}| \geq e^{-|z|/2}$. This may not seem like particularly bad behavior, and it isn't. The reason such values of λ are in the spectrum is because $(\lambda - \mathcal{L})$ has a nontrivial kernel there, so it isn't one-to-one and $(\lambda - \mathcal{L})^{-1}$ is not well defined as an operator from $L^2(\mathbb{R})$ to itself. However, as an integral kernel it's still pretty well behaved. Thus, as far as choosing the contour Γ, one really only needs to worry about the pole and the branch cut; one could, in principle, allow the contour to move through the other parts of the spectrum.

This example is simple enough that we can solve explicitly for the pointwise Greens function to find

$$\begin{aligned}\mathcal{G}(x,y,t) &= -\frac{1}{2}u_x^*(x)\left[\operatorname{errfn}\left(\frac{x-y+t}{\sqrt{4t}}\right) - \operatorname{errfn}\left(\frac{x-y-t}{\sqrt{4t}}\right)\right] \\ &\quad +\frac{1}{2}\left(1+\tanh\left(\frac{x}{2}\right)\right)\frac{1}{\sqrt{4\pi t}}e^{-\frac{(x-y+t)^2}{4t}} + \frac{1}{2}\left(1-\tanh\left(\frac{x}{2}\right)\right)\frac{1}{\sqrt{4\pi t}}e^{-\frac{(x-y-t)^2}{4t}},\end{aligned} \tag{2.3}$$

where $\operatorname{errfn}(z) = (1/\sqrt{\pi})\int_{-\infty}^{z} e^{-s^2}\mathrm{d}s$. The Greens function can be understood as follows. The first piece containing the error functions, which does not decay in time, comes from the eigenvalue at zero. It is like a generalization of a spectral projection. The error functions form an outwardly moving plateau of height 1. In the limit as $t \to \infty$, integrating the initial data against this term only leads to

$$-\frac{1}{2}u_x^*(x)\int_{\mathbb{R}} p(y,0)\mathrm{d}y.$$

The reason for the factor $-1/2$ is that $\int u_x^*(y)\mathrm{d}y = -2$, so this is just a normalization factor. The remaining two pieces look like advected heat kernels. They correspond to the fact that

$$\lim_{x\to\pm\infty} \mathcal{L} = \partial_x^2 \mp \partial_x.$$

The heat kernels get turned on and off at the appropriate ends of the real line by the factors $(1/2)(1 \pm \tanh(x/2))$. These pieces give the algebraic decay that results from the essential spectrum.

In general, one will not have an explicit formula for the resolvent kernel or the Greens function. However, one can often obtain fairly detailed pointwise bounds on the resolvent kernel that, combined with a clever choice of the contour Γ (see [ZH98]), can be used via the representation (2.1) to prove that the Greens function can be decomposed into a nondecaying piece, coming from any eigenvalues on the imaginary axis, plus a piece that decays algebraically like a heat kernel (if one has parabolic essential spectrum that touches the imaginary axis).

2.2 Main idea at the nonlinear level

The reason why pointwise estimates are so useful is because they can allow for stability results at the nonlinear level. To illustrate this, consider Burgers equation again,

$$u_t = u_{xx} - uu_x, \qquad x \in \mathbb{R}, \tag{2.4}$$

but this time let's consider the stability of $u^*(x) = 0$. (If we apply the Ansatz $u(x,t) = 0 + p(x,t)$, we just get back the original equation, above, so we will work directly with the original equation.) One way to represent solutions is via Duhamel's formula,

$$u(t) = e^{\partial_x^2 t}u(0) - \int_0^t e^{\partial_x^2(t-s)}u(s)u'(s)\mathrm{d}s.$$

However, as mentioned above, the best bound we can hope to have for the semigroup is $\|e^{\partial_x^2 t}\| \leq C$, and this will make it difficult to prove anything about decay in u via the above formula. (Of course one could prove that u decays via energy estimates, but the point here is to illustrate what can be gained by using pointwise estimates.) The pointwise representation of solutions is given by

$$u(x,t) = \int_{\mathbb{R}} \frac{1}{\sqrt{4\pi t}} e^{-\frac{(x-y)^2}{4t}} u(y,0)\mathrm{d}y - \int_0^t \int_{\mathbb{R}} \frac{1}{\sqrt{4\pi(t-s)}} e^{-\frac{(x-y)^2}{4(t-s)}} u(y,s)u_y(y,s)\mathrm{d}y\mathrm{d}s. \tag{2.5}$$

Using the convolution estimate $\|\mathcal{G} * f\|_{L^p} \leq C\|\mathcal{G}\|_{L^q}\|f\|_{L^r}$, where $1/p + 1 = 1/q + 1/r$, one can prove the following.

Lemma 2.1. *The solution to* (2.4) *satisfies*

$$\|u(t)\|_{L^p(\mathbb{R})} \leq \frac{C\|u(0)\|_{L^1(\mathbb{R})}}{t^{\frac{(p-1)}{2p}}}, \qquad t \geq 0,$$

for $1 < p < \infty$*, if the initial data is sufficiently small.*

Proof. Integrate by parts in the second term of (2.5) and multiply the entire equation by $t^{\frac{(p-1)}{2p}}$. Then take the L^p norm of each term to obtain

$$t^{\frac{(p-1)}{2p}}\|u(t)\|_{L^p} \leq C\|u(0)\|_{L^1} + Ct^{\frac{(p-1)}{2p}} \int_0^t \frac{1}{(t-s)^{\frac{(2q-1)}{2q}}} \|u^2(s)\|_{L^r}\mathrm{d}s,$$

where $1/p + 1 = 1/q + 1/r$. Now choose $r = p/2$, which forces $q = p/(p-1)$. Also, define

$$|||u|||_T = \sup_{0\leq t\leq T} t^{\frac{(p-1)}{2p}}\|u(t)\|_{L^p},$$

where T is the maximal time such that $|||u|||_T \leq 1/(2C_2)$, for a constant C_2 to be defined below. We then have

$$\begin{aligned} |||u|||_T &\leq C\|u(0)\|_{L^1} + C|||u|||_T^2 T^{\frac{(p-1)}{2p}} \int_0^T \frac{1}{(T-s)^{\frac{(p+1)}{2p}} s^{\frac{(p-1)}{p}}}\mathrm{d}s \\ &= C\|u(0)\|_{L^1} + C|||u|||_T^2 \int_0^1 \frac{1}{(1-z)^{\frac{(p+1)}{2p}} z^{\frac{(p-1)}{p}}}\mathrm{d}z =: C_1\|u(0)\|_{L^1} + C_2|||u|||_T^2, \end{aligned}$$

and so

$$|||u|||_T \leq \frac{C_1\|u(0)\|_{L^1}}{1 - C_2|||u|||_T} \leq 2C_1\|u(0)\|_{L^1},$$

due to the choice of T. If the initial data is such that $\|u(0)\|_{L^1} \leq 1/(4C_1C_2)$, then this is a bound that is in fact independent of T. Thus, it must be the case that $T = \infty$, and so we've proved the required estimate for initial data satisfying $\|u(0)\|_{L^1} \leq 1/(4C_1C_2)$. ∎

An additional difficulty arises if we linearize about the viscous shock (2.2). In this case, due to the eigenvalue at zero, the Greens function (2.3) does not decay as $t \to \infty$. However, if we could somehow remove the nondecaying piece of the Greens function, we'd be left essentially with heat kernels and potentially be able to proceed as above.

One way to handle this is to notice that the eigenvalue at zero is due to translation invariance. This can be seen because the associated eigenfunction is $u^*_x(x)$, and $u^*(x+\alpha) \approx u^*(x) + \alpha u^*_x(x)$. Moreover,

$$\lim_{t\to\infty} \int_{\mathbb{R}} \mathcal{G}(x,y,t)p(y,0)\mathrm{d}y = -\frac{1}{2}u^*_x(x) \int_{\mathbb{R}} p(y,0)\mathrm{d}y = \alpha u^*_x(x), \qquad \alpha = -\frac{1}{2}\int_{\mathbb{R}} p(y,0)\mathrm{d}y.$$

Thus, if we make the Ansatx $u(x,t) = u^*(x) + p(x,t)$, we can't expect p to decay to zero. We can, however, adjust the Ansatz to account for this expected translation and instead define

$$u(x+\alpha(t),t) = u^*(x) + p(x,t)$$

for some unknown function $\alpha(t)$ to be determined later. Plugging this into (2.4), we find

$$p_t = \mathcal{L}p - pp_x + \dot{\alpha}(u^*_x + p_x), \qquad \mathcal{L}p = p_{xx} + \tanh\left(\frac{x}{2}\right)p_x + \frac{1}{2}\mathrm{sech}^2\left(\frac{x}{2}\right)p. \tag{2.6}$$

Let's now also factor out the nondecaying part of the Greens function by writing (2.3) as

$$\mathcal{G}(x,y,t) = u^*_x(x)\mathcal{E}(y,t) + \tilde{\mathcal{G}}(x,y,t), \qquad \mathcal{E}(y,t) := -\frac{1}{2}\left[\mathrm{errfn}\left(\frac{-y+t}{\sqrt{4t}}\right) - \mathrm{errfn}\left(\frac{-y-t}{\sqrt{4t}}\right)\right].$$

One can prove that $\tilde{\mathcal{G}} := \mathcal{G} - u^*_x\mathcal{E}$ decays at least as fast as heat kernels. Since $u^*_x(x)$ is a stationary solution of the linearized equation,

$$\int_{\mathbb{R}} \mathcal{G}(x,y,t)u^*_x(y)\mathrm{d}y = u^*_x(x).$$

As a result, applying Duhamel's formula to (2.6), we find

$$\begin{aligned}
p(x,t) &= \int_{\mathbb{R}} \left[u^*_x(x)\mathcal{E}(y,t) + \tilde{\mathcal{G}}(x,y,t)\right] p(y,0)\mathrm{d}y \\
&\qquad + \int_0^t \int_{\mathbb{R}} \left[u^*_x(x)\mathcal{E}(y,t-s) + \tilde{\mathcal{G}}(x,y,t-s)\right] [(\dot{\alpha}(s) - p(y,s))p_y(y,s)]\mathrm{d}y\mathrm{d}s \\
&\qquad + \int_0^t \dot{\alpha}(s) \int_{\mathbb{R}} \mathcal{G}(x,y,t-s)u^*_x(y)\mathrm{d}y\mathrm{d}s \\
&= \int_{\mathbb{R}} \left[u^*_x(x)\mathcal{E}(y,t) + \tilde{\mathcal{G}}(x,y,t)\right] p(y,0)\mathrm{d}y \\
&\qquad + \int_0^t \int_{\mathbb{R}} \left[u^*_x(x)\mathcal{E}(y,t-s) + \tilde{\mathcal{G}}(x,y,t-s)\right] [(\dot{\alpha}(s) - p(y,s))p_y(y,s)]\mathrm{d}y\mathrm{d}s \\
&\qquad + [\alpha(t) - \alpha(0)]u^*_x(x).
\end{aligned}$$

If we now choose α to be the solution of

$$\alpha(t) := \alpha(0) - \int_{\mathbb{R}} \mathcal{E}(y,t)p(y,0)\mathrm{d}y - \int_0^t \int_{\mathbb{R}} \mathcal{E}(y,t-s)[(\dot{\alpha}(s) - p(y,s))p_y(y,s)]\mathrm{d}y\mathrm{d}s, \tag{2.7}$$

then the evolution of the perturbation is governed by

$$p(x,t) = \int_{\mathbb{R}} \tilde{\mathcal{G}}(x,y,t)p(y,0)\mathrm{d}y + \int_0^t \int_{\mathbb{R}} \tilde{\mathcal{G}}(x,y,t-s)[(\dot{\alpha}(s) - p(y,s))p_y(y,s)]\mathrm{d}y\mathrm{d}s, \tag{2.8}$$

which involves only the decaying part of the Green's function. Of course, one needs to prove that a solution to the system (2.7) - (2.8) exists, that $\alpha \to \alpha_\infty$ as $t \to \infty$, and that p decays to zero algebraically fast as $t \to \infty$, but this can now be done with nonlinear estimates similar to those described above when studying decay towards zero for Burgers equation. For more details see [Zum11].

Remark 2.2. *A key step in using pointwise estimates to prove stability is to obtain sufficient (algebraic) decay estimates on the Greens function. This step was not needed in the example, above, because we had explicit formulas for the Greens function. Typically such estimates are obtained via bounds on the resolvent kernel and the contour integral representation. This step will be crucial in the applications described below. We do not, however, have time to describe the details here. See [ZH98], [BSZ10], and [BNSZ14] for details.*

3 Two applications

We now describe two applications of the above method: time-periodic shocks in viscous conservation laws and source defects in reaction diffusion equations.

3.1 Time-periodic shocks

All of the results described in this section are based on [BSZ10]. Consider the viscous conservation law

$$u_t = u_{xx} - (f(u))_x, \qquad x \in \mathbb{R}, \qquad u \in \mathbb{R}^n. \tag{3.1}$$

Consider a time-periodic shock, which is a solution $u^*(x,t)$ of the form

$$u^*(x, t + 2\pi) = u^*(x,t), \qquad \lim_{x \to \pm\infty} u^*(x,t) = u^*_\pm,$$

where the end states $u^*_\pm$ are independent of t. (The period can always be normalized to be 2π.) This is a profile similar to the viscous shock considered above for Burgers equation, but the interior of the wave is allowed to vary periodically in time. In [TZ05, TZ08] it was shown that such solutions can result from Hopf bifurcations of stationary viscous shocks. Furthermore, in [SS08] it was shown that, if the Hopf bifurcation is supercritical, then the wave is spectrally stable, whereas if it is subcritical then the wave is unstable. The goal in [BSZ10] was to prove that a spectrally stable solution of the above form is nonlinearly stable.

If we linearize the above equation about the time-periodic shock, we find

$$p_t = p_{xx} - (f_u(u^*(x,t))p)_x =: \mathcal{L}(t)p \tag{3.2}$$

The key issue is that, since the linear operator explicitly depends on time, neither the resolvent operator or the semigroup are well-defined in the usual sense. Thus, it's not clear how to obtain good bounds on the action of the resolvent operator (or some time-dependent version of it), or how to use a contour integral to transfer that information to the linear evolution. As a result, the key theoretical advancements for this application were the formulation of and bounds for the resolvent kernel, and the development of a contour integral representation that allows for bounds of the Greens function. Once that is complete, the nonlinear stability analysis follows in a manner very similar to that described above for the stationary viscous shock of Burgers equation.

In order to understand the linear evolution, we first recall that, for time-periodic operators, the appropriate notion of spectrum is Floquet spectrum. (This is analogous with time–periodic linear ODEs.) To that end, we seek solutions of (3.2) of the form

$$e^{\sigma t} p(x,t), \qquad p(x,t) = p(x, t + 2\pi),$$

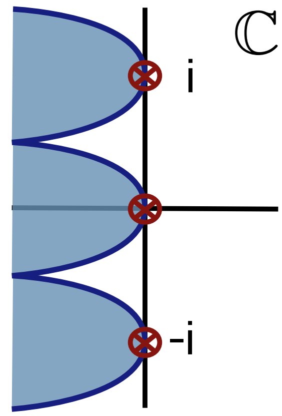

Figure 3: Floquet spectrum of a spectrally stable viscous shock near the origin. Note the spectrum is non-unique, as it can be shifted by any integer multiple of $2\pi\mathrm{i}$, and hence the parabolas repeat infinitely many times up and down the imaginary axis. There are two embedded eigenvalues at the origin, due to translations in space and time.

where σ is known as the Floquet exponent and $e^{2\pi\sigma}$ is the Floquet multiplier. Floquet exponents are not unique, as the map $\sigma \to \sigma + 2\pi\mathrm{i}$ doesn't change the Floquet multiplier. Hence, we restrict our attention to $-1/2 < \mathrm{Im}\sigma \leq 1/2$. As a result, the analogue of the spectral equation $\mathcal{L}p = \lambda p$ is given by

$$p_t + \sigma p = \mathcal{L}(t)p, \qquad p(t+2\pi) = p(t),$$

and the resolvent kernel $G(x, y, \sigma, t, s)$ must satisfy

$$G_t + \sigma G - \mathcal{L}(t)G = \delta(x-y)\delta(t-s). \tag{3.3}$$

The reason for the additional factor of $\delta(t-s)$ is that this kernel must now be allowed to depend on time. One could then seek to define the Greens function via a contour integral as follows:

$$\mathcal{G}(x, y, t, s) = \frac{1}{2\pi\mathrm{i}} \int_{-\frac{1}{2}\mathrm{i}}^{\frac{1}{2}\mathrm{i}} e^{\sigma t} G(x, y, \sigma, t, s)\mathrm{d}\sigma. \tag{3.4}$$

However, at the moment, equations (3.3)-(3.4) are a bit formal, because it's not clear that well-defined solutions to these equations exist. Justifying this formulation was one of the main results in [BSZ10].

The following three assumptions were made about the underlying shock.

- (H1) $u^*(x,t)$ is a Lax shock.
- (H2) $u^*(x,t)$ is spectrally stable, meaning that its Floquet spectrum is as depicted in Figure 3. There is no spectrum in the closed right half plane except for the double eigenvalue at the origin (and any any integer multiple of $2\pi\mathrm{i}$), with eigenfunctions u^*_x and u^*_t, which correspond to space and time translations, respectively. Moreover, this spectrum must be minimal, which would roughly correspond to having algebraic multiplicity two in the time-independent case.

For the precise statements of these assumptions, please see [BSZ10]. The first assumption is not necessary, but it made some aspects of the analysis simpler. Nonlinear stability analysis for other types of stationary shocks, such as under- and overcompressive shocks, has been carried out in [HZ06], and a similar analysis is expected to work in the time-periodic setting. The second assumption is necessary. It ensure there are no unstable eigenvalues in the right half plane, which would lead to exponential growth of perturbations, and that no algebraic growth can result from the spectrum on the imaginary axis. Under these assumptions, one can prove the following theorems.

Theorem 1. *Make the assumptions described above and pick $\rho \geq 0$. Spectral stability is equivalent to linearized stability in $L^1 \cap H^\rho$. That is, each solution of $p_t = \mathcal{L}(t)p$ with initial data in $L^1 \cap H^\rho$ converges in this space to* $\operatorname{Span}\{u_x^*, u_t^*\}$ *as $t \to \infty$.*

This theorem follows by proving that the Greens function has a decomposition similar to that described above for the linearization of Burgers equation about the viscous shock. There are pieces that do not decay, corresponding to the eigenvalues at zero, while the other pieces decay essentially like heat kernels.

Theorem 2. *Define the weighted norm $\|p\|_{H^3_w} := \|(1+x^2)^{\frac{3}{4}}p\|_{H^3}$. Under the above assumptions, u^* is nonlinearly stable with respect to initial perturbations p_0 for which $\|p_0\|_{H^3_w}$ is sufficiently small. More precisely, there exist constants $C > 0$ and $\delta > 0$ such that, for each p_0 with $\|p_0\|_{H^3_w} < \delta$, there exist functions $(q,\tau)(t)$ and constants (q_*,τ_*) so that, for all $x \in \mathbb{R}$ and $t \geq 0$, we have*

$$\|u(\cdot,t) - u^*(\cdot - q_* - q(t), t - \tau_* - \tau(t))\|_{L^r} \leq C\|p_0\|_{H^3_w}(1+t)^{-\frac{1}{2}(1-\frac{1}{r})}, \quad 1 \leq r \leq \infty,$$

where $u(x,t)$ is the solution to (3.1) *with initial data $u^*(x,0) + p_0(x)$ and*

$$|(q_*,\tau_*)| + (1+t)^{\frac{1}{2}}|(q,\tau)(t)| + (1+t)|(\dot{q},\dot{\tau})(t)| \leq C\|p_0\|_{H^3_w}.$$

Essentially, this theorem states that, for initial data sufficiently close to the underlying time-periodic wave, solutions to the full nonlinear equation (3.1) will converge to an appropriate space and time translate of the wave. Detailed bounds on the resolvent kernel and Greens function were also obtained; see [BSZ10] for details.

We now briefly describe some of the key steps in the proofs of these theorems. As mentioned above, Theorem 1 follows by obtaining an appropriate decomposition of the Greens function, and this in turn follows from sufficient bounds on the resolvent kernel and the representation (3.4). To do this, first write (3.3) as a first-order system:

$$\frac{d}{dx}\begin{pmatrix} G \\ G_x \end{pmatrix} = \mathcal{A}(x,\sigma)(t)\begin{pmatrix} G \\ G_x \end{pmatrix} + \begin{pmatrix} 0 \\ -\delta(x-y)\delta(t-s) \end{pmatrix}, \qquad \mathcal{A}(x,\sigma)(t) = \begin{pmatrix} 0 & 1 \\ \partial_t + \sigma + f_{uu}(u^*, u_x^*) & f_u(u^*) \end{pmatrix}. \tag{3.5}$$

One would like to solve this system using exponential dichotomies, which were developed for similar time-dependent systems in [SS01]. This theory would allow us to solve for $G(x,y,\sigma,\cdot,s) \in H^{m+1/2}(S^1)$ for any $m \geq 0$. We could not apply this theory directly to the above equation, however, because of the lack of smoothness in $\delta(t-s)$. (The lack of smoothness in space, via $\delta(x-y)$, had already been handled.) Addressing this issue was one main component of the proof.

Once it was shown that the resolvent kernel exists as a solution to (3.5), the issue was deriving sufficient bounds on the resolvent kernel, justifying the representation (3.4), and using it to obtain detailed bounds

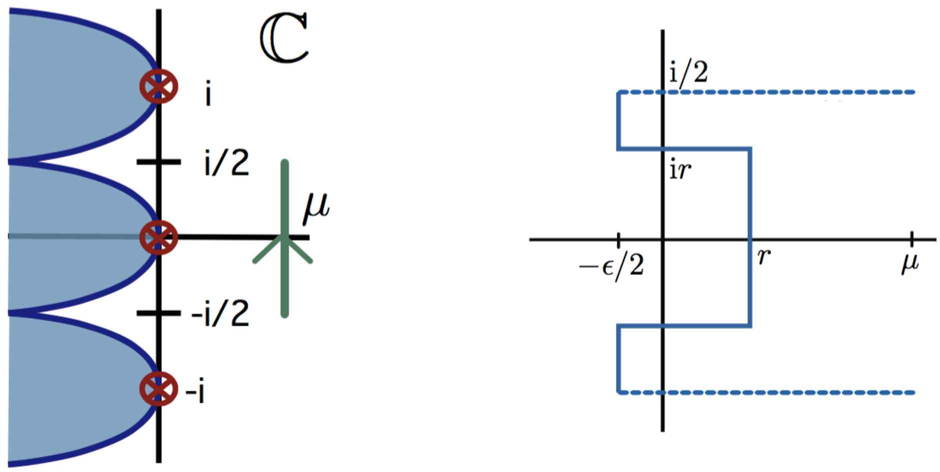

Figure 4: Left panel: original vertical contour with real part μ used in (3.4). Right panel: deformed contour used to obtain bounds on the Greens function. The parameters ϵ and r can be chosen to be small and to optimize the resultant bounds.

for the Greens function. Bounds on the resolvent kernel are obtained via the asymptotic limits

$$\lim_{x\to\pm\infty} \mathcal{A}(\sigma, x) := \mathcal{A}_\pm(\sigma) = \begin{pmatrix} 0 & 1 \\ \partial_t + \sigma & f_u(u_\pm^*) \end{pmatrix}.$$

The spectrum of this operator (which is infinite-dimensional, essentially because of the ∂_t term) will determine the spatial decay rates of the resolvent kernel. To understand this spectrum, think above expanding in Fourier space in t, so that $\partial_t \to ik$. For $k = 0$, the eigenvalues are roots of the polynomial

$$\det(\nu^2 - f_u(u_\pm^*)\nu - \sigma) = 0.$$

Some of these eigenvalues are "weak" in the sense that, when $\sigma = 0$ (which is near the part of the Floquet spectrum of $\mathcal{L}(t)$ that we're interested in), the spatial eigenvalues ν have zero real part. This causes weak decay of the resolvent kernel at spatial infinity, which is exactly the sort of behavior that's associated with the presence of the essential Floquet spectrum. By obtaining an expansion of the resolvent kernel that captures this weak spatial decay, we will be able to obtain precise bounds on the Greens function. (Parts of the resolvent kernel that decay strongly at spatial infinity will lead to higher order terms that are not as important for the estimates.)

To transfer the resolvent bounds to the Greens function via (3.4), one first has to show that contour integral is well-defined and convergent. See [BSZ10] for details. Once that is done, bounds for the Greens function can be obtained by deforming the contour Γ into the essential spectrum as shown in figure 4. This use of a vertical contour and its deformation is similar to [MZ03]. The integration over the two dotted horizontal lines cancel, so they do not create any spurious contributions to the Greens function.

Once sufficient bounds for the Greens function are obtained, the nonlinear stability analysis proceeds in a manner very similar to that described above for Burgers equation. The only modifications are due to the fact that there are now two nondecaying pieces,

$$\mathcal{G}(x, y, t, s) = u_x^*(x, t)\mathcal{E}_1(y, t, s) + u_t^*(x, t)\mathcal{E}_2(y, t, s) + \tilde{\mathcal{G}}(x, y, t, s),$$

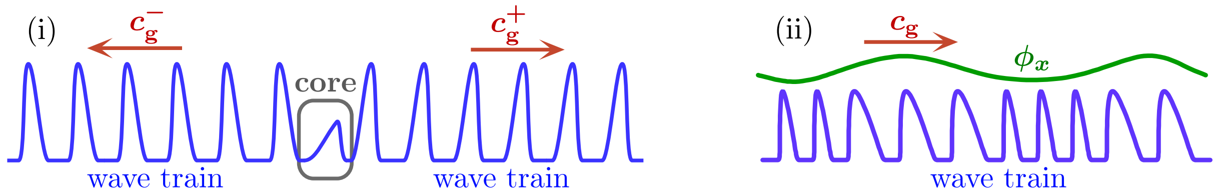

Figure 5: On the left is a diagram of the profile of a source as a function of x for a fixed value of t, with the motion of perturbations, relative to the speed of the defect core, indicated by the red arrows and the group velocities of the asymptotic wave trains. The right panel shows the behavior of small phase ϕ or wave number ϕ_x perturbation of a wave train: to leading order, they are transported with speed given by the group velocity c_g without changing their shape [DSSS09].

due to the double eigenvalue at $\sigma = 0$. To account for this, one must use an Ansatz that allows for translation in both space and time, but the main ideas of the argument are the same. See [BSZ10] for details.

3.2 Source defects in reaction-diffusion equations

Unlike the previous application, where the main mathematical difficulty occurred at the linear level, due to the time-periodicity of the operator, the main difficulty here will appear at the nonlinear level.

A defect is a solution $u_{\rm d}(x,t)$ of a reaction-diffusion equation

$$u_t = Du_{xx} + f(u), \qquad u : \mathbb{R} \times \mathbb{R}^+ \to \mathbb{R}^n \tag{3.6}$$

that is time-periodic in an appropriate moving frame $\xi = x - c_{\rm d}t$, where $c_{\rm d}$ is the speed of the defect, and spatially asymptotic to wave trains, which have the form $u_{\rm wt}(kx - \omega t; k)$ for some profile $u_{\rm wt}(\theta; k)$ that is 2π-periodic in θ. Thus, k and ω represent the spatial wave number and the temporal frequency, respectively, of the wave train. Wave trains typically exist as one-parameter families, where the frequency $\omega = \omega_{\rm nl}(k)$ is a function of the wave number k. The function $\omega_{\rm nl}(k)$ is referred to as the nonlinear dispersion relation, and its domain is typically an open interval. The group velocity $c_{\rm g}(k_0)$ of the wave train with wave number k_0 is defined as

$$c_{\rm g}(k_0) := \frac{{\rm d}\omega_{\rm nl}}{{\rm d}k}(k_0).$$

The group velocity is important as it is the speed with which small localized perturbations of the wave train propagate as functions of time, and we refer to [DSSS09] for a rigorous justification of this.

Defects have been observed in a wide variety of experiments and reaction-diffusion models and can be classified into several distinct types that have different existence and stability properties [vSH92, vH98, SS04]. This classification involves the group velocities $c_g^\pm := c_g(k_\pm)$ of the asymptotic wave trains, whose wavenumbers are denoted by $k_\pm$. Sources are defects for which $c_{\rm g}^- < c_{\rm d} < c_{\rm g}^+$, so that perturbations are transported away from the defect core towards infinity. Generically, sources exist for discrete values of the asymptotic wave numbers $k_\pm$, and in this sense they actively select the wave numbers of their asymptotic wave trains. Thus, sources can be thought of as organizing the dynamics in the entire spatial domain; their dynamics are inherently not localized. See Figure 5.

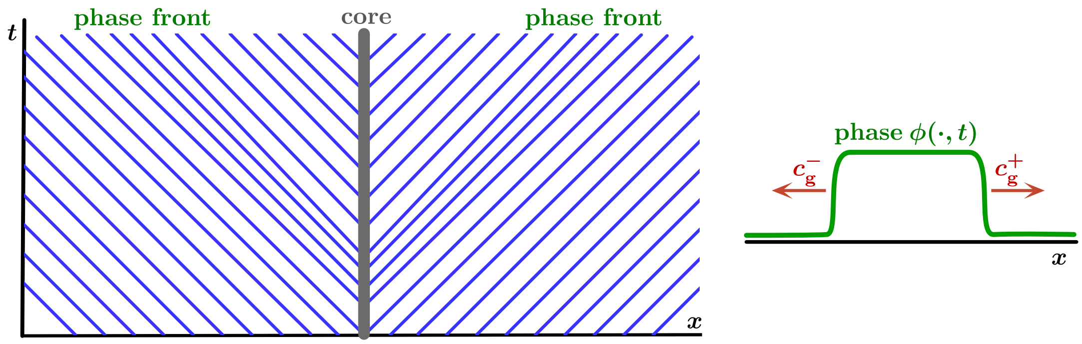

Figure 6: On the left is a sketch of the space-time diagram of a perturbed source. The defect core will adjust in response to an imposed perturbation (although this is not depicted), and the emitted wave trains, whose maxima are indicated by the lines that emerge from the defect core, will therefore exhibit phase fronts that travel with the group velocities of the asymptotic wave trains away from the core towards $\pm\infty$. The right panel illustrates the profile of the anticipated phase function $\phi(x, t)$.

When analyzing the stability of a source, there are several key difficulties. First, since they are time-periodic, the linearized operator $\mathcal{L}(t)$ will be time-periodic, and spectrally stable sources will have a spectral picture similar to the time-periodic shocks [SS04]. This is a difficulty we now know how to deal with, due to the previous example [BSZ10]. Second, since we will be linearizing (3.6) about the source, rather than linearizing (3.1) as in the previous case, we will not have the conservation law structure, $(f(u))_x$, in the nonlinear term. This x-derivative is useful because in Duhamel's formula we can integrate by parts and transfer that derivative to the Greens function, thus creating extra temporal decay, which helps close the nonlinear argument. Since this is not possible for reaction-diffusion equations, the nonlinear estimates become more delicate. The final difficulty is that, since we will linearize about a source, its asymptotic wave trains will send any perturbation, even if it is initially localized, out towards spatial infinity. Thus, the perturbation will not stay localized. This will add an additional degree of delicacy to the nonlinear estimates. Moreover, this property of the source will also change the structure of the Greens function, due to the fact that the eigenfunctions associated with the zero eigenvalue will no longer be spatially localized. The corresponding adjoint eigenfunctions will be exponentially localized in space, however, which implies that the source has a well defined spatial position and temporal phase.

If a source is subjected to a localized perturbation, then one anticipated effect is that the defect core adjusts its position and its temporal phase in response. From its new position, the defect will continue to emit wave trains with the same selected wave number, but there will now be a phase difference between the asymptotic wave trains at infinity and those newly emitted near the core. In other words, we expect to see two phase fronts that travel in opposite directions away from the core as illustrated in Figure 6. The resulting phase dynamics can be captured by writing the perturbed solution $u(x, t)$ as

$$u(x, t) = u_d(x, t + \phi(x, t)) + p(x, t),$$

where we expect that the perturbation $p(x, t)$ of the defect profile decays in time, while the phase $\phi(x, t)$ resembles an expanding plateau as indicated in Figure 6 whose height depends on the initial perturbation through the spatio-temporal displacement of the defect core.

Initially, to simplify the analysis, we focused only on the analysis of the dynamics of the phase ϕ. For phase perturbations of wave trains, it was indeed established formally in [HK77] and proved rigorously in [DSSS09] that the phase $\phi(x,t)$ satisfies an integrated Burgers equation for long times. This lead us to consider in [BNSZ12] the model problem

$$\phi_t = \phi_{xx} - c\tanh\left(\frac{cx}{2}\right)\phi_x + \phi_x^2, \qquad c > 0 \tag{3.7}$$

with small localized initial data, where $x \in \mathbb{R}$, $t > 0$, and $\phi(x,t)$ is a scalar function representing the phase. This equation is related to the linearization of Burgers equation about the viscous shock, (2.2), with some key differences. First, the sign of the advection term is negative, rather than positive, which directs the motion of the perturbation outward, rather than inward. The parameter c represents the speed of the perturbation, so we are effectively assuming for simplicity that $c_d = 0$ and $c_g^- = -c < 0 < c = c_g^+$. Second, the equation has been integrated, which is consistent with the above-mentioned results [HK77, DSSS09] on phase perturbations of wave trains. This removes the $\mathrm{sech}^2(cx/2)$ term, changes the nonlinearity from pp_x to p^2, and replaces p with ϕ_x. One effect of this is to remove the zero eigenvalue from the spectrum of the linear operator, which is otherwise the same as for the operator in (2.2). Having an embedded zero eigenvalue is a difficulty that one can deal with, as described above, and so this allows us to focus on the third difficulty, mentioned above, of the outward motion of the perturbations. The following theorem was proven in [BNSZ12].

Theorem 3. *For each $\gamma \in (0, \frac{1}{2})$, there exist constants $\epsilon_0, \eta_0, C_0, M_0 > 0$ such that the following is true. If $\phi_0 \in C^1$ satisfies*

$$\epsilon := \|\mathrm{e}^{x^2/M_0}\phi_0\|_{C^1} \le \epsilon_0$$

then the solution $\phi(x,t)$ of (3.7) with $\phi(\cdot,0) = \phi_0$ exists globally in time and can be written in the form

$$\phi(x,t) = \phi^*(x,t,\alpha(t)) + p(x,t)$$

for appropriate functions $\alpha(t)$ and $p(x,t)$, and with $\phi^*(x,t,\alpha) := \log\left(1 + \alpha\mathcal{G}(x,0,t)\right)$, where $\mathcal{G}$ is the Greens function for the linear operator in (3.7). Furthermore, there is an $\alpha_\infty \in \mathbb{R}$ with $|\alpha_\infty| \le C_0$ such that

$$|\alpha(t) - \alpha_\infty| \le \epsilon C_0 \mathrm{e}^{-\eta_0 t},$$

and $p(x,t)$ satisfies

$$|p(x,t)| \le \frac{\epsilon C_0}{(1+t)^\gamma}\left(\mathrm{e}^{-\frac{(x+ct)^2}{M_0(t+1)}} + \mathrm{e}^{-\frac{(x-ct)^2}{M_0(t+1)}}\right), \quad |p_x(x,t)| \le \frac{\epsilon C_0}{(1+t)^{\gamma+1/2}}\left(\mathrm{e}^{-\frac{(x+ct)^2}{M_0(t+1)}} + \mathrm{e}^{-\frac{(x-ct)^2}{M_0(t+1)}}\right)$$

for all $t \ge 0$. In particular, $\|p(\cdot,t)\|_{L^r} \to 0$ as $t \to \infty$ for each fixed $r > \frac{1}{2\gamma}$.

This theorem essentially says that the solution to (3.7) looks like an outwardly expanding plateau, given by ϕ^*, plus a perturbation that decays like a Gaussian. One can explicitly determine a formula for the Greens function $\mathcal{G}$. The reason for the form of ϕ^* is that, if α were constant, this would be an exact solution of (3.7) by the Cole-Hopf transformation. However, we need to let the height of the plateau $\alpha(t)$ vary so as to remove the non-decaying part of the Green's function before conducting the nonlinear estimates. In other words, the key mathematical advancement of this results was to determine the appropriate Ansatz for the form of solutions, $\phi(x,t) = \phi^*(x,t,\alpha(t)) + p(x,t)$, so as to enable removal of the non-decaying part of the Green's function and closure of the nonlinear estimates. For more details see [BNSZ12].

Once the toy model was analyzed, and it was understood how to handle the non-localization of perturbations, the next step [BNSZ14] was to analyze the nonlinear stability of sources in the complex cubic-quintic Ginzburg-Landau (qCGL) equation

$$A_t = (1+i\tilde{\alpha})A_{xx} + A - (1+i\beta)A|A|^2 + (\gamma_1 + i\gamma_2)A|A|^4. \tag{3.8}$$

Here $A = A(x,t)$ is a complex-valued function, $x \in \mathbb{R}$, $t \geq 0$, and $\tilde{\alpha}, \beta, \gamma_1$, and γ_2 are all real constants with $\gamma = \gamma_1 + i\gamma_2$ being small but nonzero. (The reason for the tilde above α is to distinguish it from the α which has been used, and will continue to be used, to denote an initially arbitrary function that will be chosen to remove non-decaying parts of the Greens function.) It is shown, for instance in [BN85, PSAK95, Doe96, KR00, Leg01, SS04], that the qCGL equation exhibits a family of sources, and in fact much detail is known about these sources. When $c_d = 0$, they have the form

$$A_{\text{source}}(x,t) = r(x)\mathrm{e}^{\mathrm{i}\varphi(x)}\mathrm{e}^{-\mathrm{i}\omega_0 t},$$

where

$$\lim_{x\to\pm\infty} \varphi_x(x) = \pm k_0, \qquad \lim_{x\to\pm\infty} r(x) = \pm r_0(k_0), \qquad \omega_0 = \omega_0(k_0),$$

and the details of the functions r and φ, as well as information about r_0 and ω_0, are known. What is particularly useful here is that the time dependence, via the term $\mathrm{e}^{-\mathrm{i}\omega_0 t}$, factors out. Therefore we can study perturbations of the amplitude and phase using an Ansatz of the form

$$A(x+\alpha(x,t),t) = (r(x) + R(x,t))\mathrm{e}^{\mathrm{i}(\phi(x)+\varphi(x,t))}e^{-\mathrm{i}\omega_0 t}$$

without ending up wtih a time-dependent linearized operator. As a result, we can now essentially focus on two of the three above-mentioned difficulties that one may encounter when analyzing the nonlinear stability of sources. Here R and φ are the amplitude and phase perturbations that we wish to prove decay in some appropriate sense, and $\alpha(x,t)$ is a function we can choose so as to cancel any non-decaying parts of the Greens function. Rather than proving this directly, we instead show that solutions converge to a modulated source defined by

$$A_{\text{mod}}(x,t) := A_{\text{source}}(x,t)\mathrm{e}^{\mathrm{i}\phi^a(x,t)} = r(x)\mathrm{e}^{\mathrm{i}(\varphi(x)+\phi^a(x,t))}\mathrm{e}^{-\mathrm{i}\omega_0 t}.$$

The functions $\alpha(x,t)$ and $\phi^a(x,t)$ together will remove from the dynamics any non-decaying or slowly-decaying terms, resulting from the zero eigenvalues and the quadratic terms in the nonlinearity, thus allowing a nonlinear iteration scheme to be closed. To describe these functions in more detail, we define

$$e(x,t) := \text{errfn}\left(\frac{x + c_{\mathrm{g}}t}{\sqrt{4\mathrm{d}t}}\right) - \text{errfn}\left(\frac{x - c_{\mathrm{g}}t}{\sqrt{4\mathrm{d}t}}\right), \qquad \text{errfn}(z) := \frac{1}{2\pi}\int_{-\infty}^{z} \mathrm{e}^{-x^2}\,dx$$

and the Gaussian-like term

$$\theta(x,t) := \frac{1}{(1+t)^{1/2}}\left(\mathrm{e}^{-\frac{(x-c_{\mathrm{g}}t)^2}{M_0(t+1)}} + \mathrm{e}^{-\frac{(x+c_{\mathrm{g}}t)^2}{M_0(t+1)}}\right),$$

where M_0 is a fixed positive constant. Now define

$$\begin{aligned}
\phi^a(x,t) &:= -\frac{\mathrm{d}}{2q}\Big[\log\Big(1+\delta^+(t)e(x,t+1)\Big) + \log\Big(1+\delta^-(t)e(x,t+1)\Big)\Big],\\
\alpha(x,t) &:= \frac{\mathrm{d}}{2qk_0}\Big[\log\Big(1+\delta^+(t)e(x,t+1)\Big) - \log\Big(1+\delta^-(t)e(x,t+1)\Big)\Big],
\end{aligned}$$

where the constant q and the smooth functions $\delta^{\pm} = \delta^{\pm}(t)$ (which are chosen to remove non-decaying parts of the Greens function) are defined in [BNSZ14]. The formulas for ϕ^a and α are related to an application of the Cole-Hopf transformation. Our main result asserts that the shifted solution $A(x+\alpha(x,t),t)$ converges to the modulated source with the decay rate of a Gaussian [BNSZ14].

Theorem 4. *Assume that the initial data is of the form $A_{\rm in}(x) = R_{\rm in}(x)e^{i\phi_{\rm in}(x)}$ with $R_{\rm in}, \phi_{\rm in} \in C^3(\mathbb{R})$. In addition, assume that $A_{\rm source}$ is spectrally stable and that certains assumptions on the parameters in* (3.8)*, which can be found in [BNSZ14, Lemma2.1], are satisfied. There exists a positive constant ϵ_0 such that, if*

$$\epsilon := \|A_{\rm in}(\cdot) - A_{\rm source}(\cdot,0)\|_{\rm in} \leq \epsilon_0,$$

then the solution $A(x,t)$ to the qCGL equation (3.8) *exists globally in time. In addition, there are constants $\eta_0, C_0, M_0 > 0$, $\delta_\infty^{\pm} \in \mathbb{R}$ with $|\delta_\infty^{\pm}| \leq \epsilon C_0$, and smooth functions $\delta^{\pm}(t)$ so that*

$$|\delta^{\pm}(t) - \delta_\infty^{\pm}| \leq \epsilon C_0 \mathrm{e}^{-\eta_0 t}, \qquad \forall t \geq 0$$

and

$$\left|\frac{\partial^\ell}{\partial x^\ell}\Big[A(x+\alpha(x,t),t) - A_{\rm mod}(x,t)\Big]\right| \leq \epsilon C_0(1+t)^\kappa[(1+t)^{-\ell/2} + e^{-\eta_0|x|}]\theta(x,t), \qquad \forall x\in\mathbb{R}, \quad \forall t \geq 0, \quad (3.9)$$

for $\ell = 0,1,2$ and for each fixed $\kappa \in (0,\frac{1}{2})$. In particular, $\|A(\cdot+\alpha(\cdot,t),t) - A_{\rm mod}(\cdot,t)\|_{W^{2,r}} \to 0$ as $t\to\infty$ for each fixed $r > \frac{1}{1-2\kappa}$.

This theorem implies that the phase $\varphi(x) + \phi(x,t)$ tends to $\varphi(x) + \phi^a(x,t)$, where $\phi^a(x,t)$ looks like an expanding plateau as time increases. The functions $\delta^{\pm}(t)$ will be constructed via integral formulas that are introduced to precisely capture the non-decaying part of the Green's function of the linearized operator. The choices of $\alpha(x,t)$ and $\phi^a(x,t)$ are made based on the fact that the asymptotic dynamics of the translation and phase variables is governed (to leading order) by a nonlinear Burgers-type equation:

$$\Big(\partial_t + \frac{c_{\rm g}}{k_0}\varphi_x\partial_x - \mathrm{d}\partial_x^2\Big)(\phi^a \pm k_0\alpha) = q(\partial_x\phi^a \pm k_0\partial_x\alpha)^2.$$

By defining α and ϕ^a in this way, we are able to remove not only the non-decaying parts of the Greens function, but also the quadratic terms in the nonlinearity. These terms (which are not present when the equation has conservation law structure, as for the time-periodic shocks) are problematic for the nonlinear estimates. This is related to the fact that the zero solution of $u_t = u_{xx} - u^2$ is unstable. See [BNSZ14] for more details.

4 Appendix

Here we present two examples of how to compute a resolve kernel. First consider the equation

$$\lambda G - G_{xx} = \delta(x-y).$$

Two solutions to the homogeneous equation $\lambda u - u_{xx} = 0$ are

$$u_+(x,\lambda) = e^{\sqrt{\lambda}x}, \qquad u_-(x,\lambda) = e^{-\sqrt{\lambda}x}.$$

We can solve for the resolvent kernel using a method known as variation of constants. Suppose the solution has the form

$$G(x,y,\lambda) = v_+(x,y,\lambda)u_+(x,\lambda) + v_-(x,y,\lambda)u_-(x,\lambda),$$

for some unknown functions $v_\pm$. Differentiating once with respect to x we find

$$G_x = \partial_x v_+ u_+ + v_+\partial_x u_+ + \partial_x v_- u_- + v_-\partial_x u_-.$$

For convenience, we force $\partial_x v_+ u_+ + \partial_x v_- u_- = 0$. This then leads to

$$G_{xx} = \partial_x v_+ \partial_x u_+ + v_+\partial_x^2 u_+ + \partial_x v_- \partial_x u_- + v_-\partial_x^2 u_-.$$

Inserting this into the above equation and using the fact that $u_\pm$ solve the homogeneous equation, we find

$$\partial_x v_+ \partial_x u_+ + \partial_x v_- \partial_x u_- = -\delta(x-y).$$

Hence, to find a solution, we must solve the system of equations

$$\begin{aligned} \partial_x v_+ u_+ + \partial_x v_- u_- &= 0 \\ \partial_x v_+ \partial_x u_+ + \partial_x v_- \partial_x u_- &= -\delta(x-y). \end{aligned}$$

This can be equivalently written as

$$\begin{pmatrix} \partial_x v_+ \\ \partial_x v_- \end{pmatrix} = \begin{pmatrix} u_+ & u_- \\ \partial_x u_+ & \partial_x u_- \end{pmatrix}^{-1} \begin{pmatrix} 0 \\ -\delta(x-y) \end{pmatrix} = \frac{1}{u_+\partial_x u_- - u_-\partial_x u_+} \begin{pmatrix} \partial_x u_- & -u_- \\ -\partial_x u_+ & u_+ \end{pmatrix} \begin{pmatrix} 0 \\ -\delta(x-y) \end{pmatrix}.$$

Using the fact, for $\lambda \notin (-\infty, 0] = \sigma(\mathcal{L})$, u_+ is well behaved at $-\infty$ and u_- is well-behaved at $+\infty$, as well as the fact that the Wronskian is given by

$$u_+\partial_x u_- - u_-\partial_x u_+ = -2\sqrt{\lambda},$$

we find that

$$\begin{aligned} -v_+(x,y,\lambda) &= \int_x^\infty \partial_x v_+(x,y,\lambda)\mathrm{d}x = -\frac{1}{2\sqrt{\lambda}}\int_x^\infty u_-(x,\lambda)\delta(x-y)\mathrm{d}x = -\frac{1}{2\sqrt{\lambda}}u_-(y,\lambda)H(y-x) \\ v_-(x,y,\lambda) &= \int_{-\infty}^x \partial_x v_-(x,y,\lambda)\mathrm{d}x = \frac{1}{2\sqrt{\lambda}}\int_{-\infty}^x u_+(x,\lambda)\delta(x-y)\mathrm{d}x = \frac{1}{2\sqrt{\lambda}}u_+(y,\lambda)H(x-y), \end{aligned}$$

where H is the Heaviside function. As a result, the resolvent kernel is given by

$$G(x,y,\lambda) = \frac{1}{2\sqrt{\lambda}}u_-(y,\lambda)u_+(x,\lambda)H(y-x) + \frac{1}{2\sqrt{\lambda}}u_+(y,\lambda)u_-(x,\lambda)H(x-y) = \frac{1}{2\sqrt{\lambda}}e^{-\sqrt{\lambda}|x-y|}.$$

Next consider the associated equation for the linearization of Burgers equation about the viscous shock:

$$\lambda u - u_{xx} - \tanh\left(\frac{x}{2}\right)u_x - \frac{1}{2}\mathrm{sech}^2\left(\frac{x}{2}\right)u = \delta(x-y).$$

The two solutions to the homogeneous equation are given by

$$u_\pm(x,\lambda) = \left(-\frac{1}{2}\tanh\left(\frac{x}{2}\right) \pm \sqrt{\lambda+\frac{1}{4}}\right)\mathrm{sech}\left(\frac{x}{2}\right)e^{\pm\sqrt{\lambda+\frac{1}{4}}x}.$$

These can be found by using the changes of variables $v = \int_{-\infty}^x u$ followed by $w = \cosh(x/2)v$, which transforms the homogeneous equation into $w_{xx} - (\lambda + 1/4)w = 0$. Now one can use the method of variation of constants, as above, to solve for the resolvent kernel, which is given above in §2.1.

References

[BN85] N Bekki and B. Nozaki. Formations of spatial patterns and holes in the generalized Ginzburg-Landau equation. *Phys. Lett. A*, 110:133–135, 1985.

[BNSZ12] M. Beck, T. Nguyen, B. Sandstede, and K. Zumbrun. Toward nonlinear stability of sources via a modified Burgers equation. *Phys. D*, 241:382–392, 2012.

[BNSZ14] Margaret Beck, Toan T. Nguyen, Björn Sandstede, and Kevin Zumbrun. Nonlinear stability of source defects in the complex Ginzburg-Landau equation. *Nonlinearity*, 27(4):739–786, 2014.

[BSZ10] Margaret Beck, Björn Sandstede, and Kevin Zumbrun. Nonlinear stability of time-periodic viscous shocks. *Arch. Ration. Mech. Anal.*, 196(3):1011–1076, 2010.

[Doe96] A. Doelman. Breaking the hidden symmetry in the ginzburg-landau equation. *Physica D*, 97:398–428, 1996.

[DSSS09] Arjen Doelman, Björn Sandstede, Arnd Scheel, and Guido Schneider. The dynamics of modulated wave trains. *Mem. Amer. Math. Soc.*, 199(934):viii+105, 2009.

[EN00] Klaus-Jochen Engel and Rainer Nagel. *One-parameter semigroups for linear evolution equations*, volume 194 of *Graduate Texts in Mathematics*. Springer-Verlag, New York, 2000. With contributions by S. Brendle, M. Campiti, T. Hahn, G. Metafune, G. Nickel, D. Pallara, C. Perazzoli, A. Rhandi, S. Romanelli and R. Schnaubelt.

[Hen81] D. Henry. *Geometric Theory of Semilinear Parabolic Equations*. Springer-Verlag, Berlin, 1981.

[HK77] L. N. Howard and N. Kopell. Slowly varying waves and shock structures in reaction-diffusion equations. *Studies in Appl. Math.*, 56(2):95–145, 1976/77.

[HZ06] Peter Howard and Kevin Zumbrun. Stability of undercompressive shock profiles. *J. Differential Equations*, 225(1):308–360, 2006.

[KP13] Todd Kapitula and Keith Promislow. *Spectral and dynamical stability of nonlinear waves*, volume 185 of *Applied Mathematical Sciences*. Springer, New York, 2013. With a foreword by Christopher K. R. T. Jones.

[KR00] T. Kapitula and J. Rubin. Existence and stability of standing hole solutions to complex Ginzburg-Landau equations. *Nonlinearity*, 13(1):77–112, 2000.

[Leg01] J. Lega. Traveling hole solutions of the complex Ginzburg-Landau equation: a review. *Phys. D*, 152/153:269–287, 2001. Advances in nonlinear mathematics and science.

[MZ03] Corrado Mascia and Kevin Zumbrun. Pointwise Green function bounds for shock profiles of systems with real viscosity. *Arch. Ration. Mech. Anal.*, 169(3):177–263, 2003.

[Paz83] A. Pazy. *Semigroups of linear operators and applications to partial differential equations*, volume 44 of *Applied Mathematical Sciences*. Springer-Verlag, New York, 1983.

[PSAK95] S. Popp, O. Stiller, I. Aranson, and L. Kramer. Hole solutions in the 1D complex Ginzburg-Landau equation. *Phys. D*, 84(3-4):398–423, 1995.

[SS01] B. Sandstede and A. Scheel. On the structure and spectra of modulated traveling waves. *Math. Nachr.*, 232:39–93, 2001.

[SS04] B. Sandstede and A. Scheel. Defects in oscillatory media: toward a classification. *SIAM Appl Dyn Sys*, 3(1):1–68, 2004.

[SS08] Björn Sandstede and Arnd Scheel. Hopf bifurcation from viscous shock waves. *SIAM J. Math. Anal.*, 39(6):2033–2052, 2008.

[TZ05] Benjamin Texier and Kevin Zumbrun. Relative Poincaré-Hopf bifurcation and galloping instability of traveling waves. *Methods Appl. Anal.*, 12(4):349–380, 2005.

[TZ08] Benjamin Texier and Kevin Zumbrun. Galloping instability of viscous shock waves. *Physica D*, 237:1553–1601, 2008.

[vH98] M. van Hecke. Building blocks of spatiotemporal intermittency. *Phys. Rev. Lett.*, 80:1896–1899, 1998.

[vSH92] Wim van Saarloos and P. C. Hohenberg. Fronts, pulses, sources and sinks in generalized complex Ginzburg-Landau equations. *Phys. D*, 56(4):303–367, 1992.

[ZH98] Kevin Zumbrun and Peter Howard. Pointwise semigroup methods and stability of viscous shock waves. *Indiana Univ. Math. J.*, 47(3):741–871, 1998.

[Zum11] K. Zumbrun. Instantaneous shock location and one-dimensional nonlienar stability of viscous shock waves. *Quarterly of Applied Mathematics*, 69(1):177–202, 2011.